

# Compound temperature and precipitation extreme events in southern South America: associated atmospheric circulation, and simulations by a multi-RCM ensemble

Bárbara Tencer<sup>1</sup>, María Laura Bettolli<sup>2,3,4</sup>, Matilde Rusticucci<sup>2,3,4,\*</sup>

<sup>1</sup>School of Earth and Ocean Sciences, University of Victoria, 3800 Finnerty Rd., Victoria BC V8P 5C2, Canada

<sup>2</sup>Departamento de Ciencias de la Atmósfera y los Océanos, Facultad de Ciencias Exactas y Naturales, Universidad de Buenos Aires, 2do. Piso, Pabellón II, Ciudad Universitaria C1428 EHA, Ciudad de Buenos Aires, Argentina

<sup>3</sup>CONICET, C1033AAJ, Av Rivadavia 1917, Buenos Aires, Argentina

<sup>4</sup>Instituto Franco Argentino sobre Estudios de Clima y sus Impactos (UMI IFAECI)/CNRS, UMI – IFAECI, CIMA, 2do. Piso, Pabellón II, Ciudad Universitaria (C1428EGA), Buenos Aires, Argentina

**ABSTRACT:** In this paper we analyse the joint distribution of extreme temperature and heavy precipitation events in southern South America during 1961–2000, and the predominant atmospheric circulation associated with the occurrence of compound extreme events. We show that the probability of occurrence of intense precipitation (daily rainfall higher than the 75th percentile) significantly increases during or following a warm night (minimum temperature higher than the 90th percentile), but decreases during a cold night (minimum temperature lower than the 10th percentile) during the warm season. Heavy precipitation events are associated with the simultaneous occurrence of warm days (maximum temperature higher than the 90th percentile) or following such an event in eastern Argentina, but they rarely occur before. In contrast, cold days (maximum temperature lower than the 10th percentile) happen more often after an intense rain. Compound events are usually associated with 1 or 2 typical circulation patterns in each subregion. For example, warm days and heavy precipitation tends to occur more often when a trough over the Pacific Ocean and a cold front over the continent lead to warm and wet air advected to the east of the region of study. We also analysed the skill of 7 regional climate models from the CLARIS LPB project to simulate the statistical relationship between temperature and precipitation extremes in 1990–2000. Overall, models were able to simulate an increase in the probability of occurrence of extreme rainfall during warm nights and cold days, and an inhibition of precipitation during cold nights. However, models tend to fail to capture the spatial distribution of the compound extreme events in southeastern South America.

**KEY WORDS:** Compound extremes · Extreme temperature · Heavy precipitation · Atmospheric circulation · Regional climate models

—Resale or republication not permitted without written consent of the publisher—

## 1. INTRODUCTION

Social and natural systems in Central and South America are highly influenced by climate variability at different time scales. Extreme events in particular

have impacted large areas of the American continent. During 2000–2013, 613 individual weather and climate extreme events were registered in the region, affecting more than 50 million people and leaving >13 000 fatalities and >US\$52 billion in economic

damage (Magrin et al. 2014). In addition, changes in climate variability have severely affected the region. Increasing trends in annual rainfall have been observed in southeastern South America ( $0.6 \text{ mm d}^{-1}$  during 1950–2008) and warming has been detected throughout Central and South America (near  $0.7$  to  $1^\circ\text{C}$  since the mid-1970s). Extreme events have also changed in the region during the second half of the 20th century: temperature extremes have increased in Central America and most of tropical and subtropical South America, while extreme rainfall in southeastern South America has become more frequent, leading to a higher occurrence of landslides and flash floods (see Magrin et al. 2014 and references therein).

The Intergovernmental Panel on Climate Change (IPCC) defines a compound extreme event when 2 or more extreme events occur simultaneously or consecutively, when different extreme events combined lead to an amplification of the impact of the events, or when individual events that are not extreme by themselves lead to an extreme event or impact when they occur together, leading to an emerging risk (Seneviratne et al. 2012, Reisinger et al. 2014). When a drought period is concomitant or followed by a period of extremely high temperature, the consequences for certain types of crops can be more severe than dry conditions alone (Jiang & Huang 2000). Also, fire risk increases when these 2 extreme events occur simultaneously (Bradstock et al. 2009). However, the understanding of concomitant temperature and precipitation stress and its impacts is still very poor.

A first approach to understanding the behaviour of compound temperature and precipitation extremes is based on the fact that changes observed in temperature and precipitation can be physically related. Madden & Williams (1978) and Zhao & Khalil (1993) analysed correlations between mean seasonal temperature and total precipitation in the US and Europe and found that cool summers tend to be associated with wet conditions, while droughts are usually observed together with heat waves. On a global scale, Trenberth & Shea (2005) showed a strong negative correlation between mean monthly temperature and precipitation during summer over the continents in both hemispheres, showing that summers tend to be warm and dry or cool and wet. The authors attributed this behaviour to the fact that dry conditions favour direct radiation and a lower cooling due to evaporation. However, poleward of  $40^\circ$ , winter positive correlations are stronger, since the low moisture-holding capacity of the air in cold conditions limits the amount of precipitation. In regions where oceanic

conditions are dominant, warm temperatures are usually associated with an increase in precipitation, such as during El Niño events (Trenberth et al. 2007).

In southern South America, Rusticucci & Penalba (2000) described an inverse relationship between temperature and precipitation during the warm season (December to April): warm summers were associated with low precipitation, especially in northeastern and central-western Argentina, south of Chile and in Paraguay, while cool summers were related to above-normal precipitation due to an increase in the frequency of cold fronts. More recently, based on observed monthly data, Barrucand et al. (2014) showed that warm and dry conditions were significantly more frequent than cool and dry conditions in central Argentina all year round. However, cool and dry months were predominant in the east of the country, especially after 1976.

Even though mean values and extreme events do not usually share the same distribution, Rusticucci & Barrucand (2004) showed that the occurrence of extreme temperature events and mean seasonal values are highly correlated in Argentina. During summer, correlation coefficients between the mean seasonal temperature and warm days or nights were significant and  $>0.7$  in central Argentina, indicating that an increase in mean values would lead to more frequent warm extreme events. Negative correlations of lower magnitudes were found between the summer mean temperature and cold days or nights, but almost no significant relationship was found during winter for any of the analysed extreme events.

However, very few studies have analysed the occurrence of compound extreme events. In Canada, the analysis of the joint distribution of daily extreme temperature and heavy precipitation events showed that the occurrence of these 2 types of extremes is not independent of each other (Tencer et al. 2014). The authors found a significant positive relationship between warm nights (minimum temperature above the 90th percentile) or warm days (maximum temperature above the 90th percentile) and heavy precipitation (daily precipitation above the 75th percentile), with greater frequencies of compound extreme occurrences observed in coastal areas, especially during fall and winter. During spring and summer, warm days were usually associated with an inhibition of heavy precipitation over the entire region of study. Cold days (maximum temperature below the 10th percentile) were usually associated with heavy precipitation during summertime, but the opposite relationship was observed during winter. Cold nights (minimum temperature below the 10th percentile)

were almost always associated with a decrease in the number of heavy precipitation events.

In this study, we used a similar methodology as that presented by Tencer et al. (2014) to analyse the joint occurrence of heavy precipitation and extreme temperature events in southeastern South America based on historical observations of the second half of the 20th century and the atmospheric circulation associated with these compound extremes.

The study of the relationship between extreme temperature and precipitation events can also help reduce the uncertainties associated with projected changes in extreme precipitation events in the region. The skill of both global and regional climate models (RCMs) to simulate mean and extreme precipitation in southeastern South America is not at all satisfactory (Vera et al. 2006, Solman et al. 2008, 2013, Carril et al. 2012, Bettolli & Penalba 2014). A multi-model ensemble of 4 RCMs forced by ERA-40 reanalysis for the period 1991–2000 was able to capture the large-scale precipitation over the region, but it overestimated the number of wet days and underestimated both the daily rainfall intensity and heavy precipitation events, especially during summer (Carril et al. 2012). A more recent and larger ensemble developed for the same region shows that the underestimation of wintertime precipitation over La Plata Basin is a systematic shortcoming of the models, due to their lack of skill in simulating the amplitude of the synoptic scale activity which is the main source of precipitation (Solman et al. 2013). Therefore, the understanding and quantification of a conditional probability between temperature and precipitation will allow an estimation of the probability of occurrence of heavy precipitation events, given the occurrence of an extreme temperature event. We therefore aimed to assess the capability of the regional climate models to reproduce this relationship.

## 2. DATA AND METHODOLOGY

### 2.1. Observed data

We used daily precipitation (Pr), and maximum and minimum temperature (Tx and Tn, respectively) observed at meteorological stations during the period 1961–2000 in southern South America (Fig. 1). Data were gathered and quality controlled during the

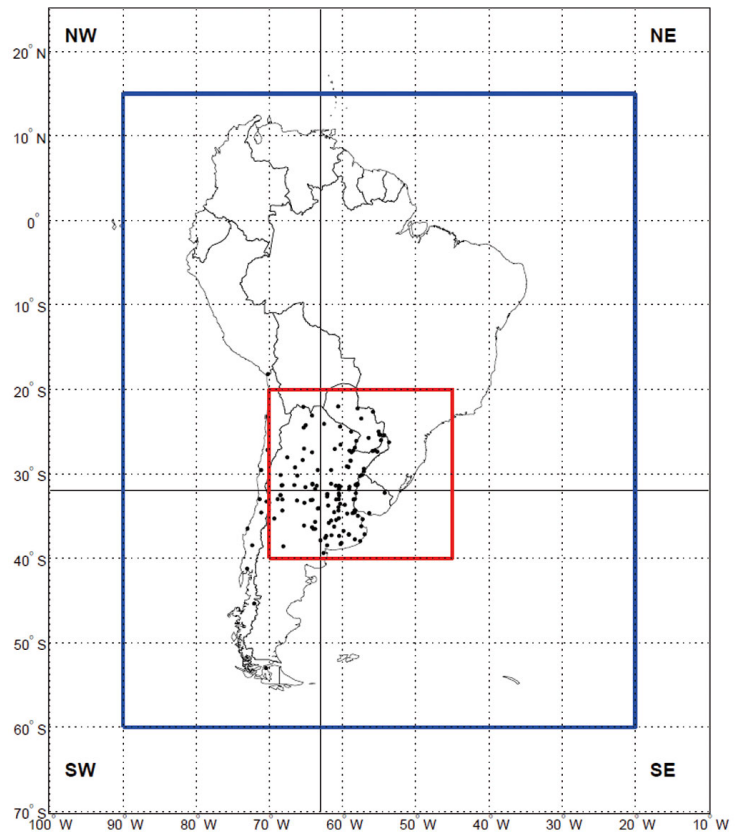


Fig. 1. Stations (black dots; period available: 1961–2000) and subregions (NE, NW, SE, SW; delineated by black lines) used in this study. Red and blue squares indicate the observed gridded dataset domain (period available: 1961–2000) and the regional climate model domain (period of simulations: 1990–2008), respectively

CLARIS LPB – ‘A Europe-South America Network for Climate Change Assessment and Impact Studies in La Plata Basin’ project (Penalba et al. 2014). The region of study was subdivided into 4 different subregions for the analysis of the patterns of circulation associated with the occurrence of compound extreme events. The 4 subregions were defined according to different climatological regimes east of the Andes (Prohaska 1976, Rusticucci & Penalba 2000). The stations located west of the Andes belong to different climate regimes. However, due to the low spatial coverage and scarce number of stations in Chile, they were not considered for the analysis of the relationship with the circulation.

Only stations with at least 20 yr of records in the period of study (1961–2000) and <10% of missing data over the whole period were used for this study, leaving a total of 143 stations in the region (24 in the NW, 46 in the NE, 27 in the SW and 46 in the SE). However, as discussed later, not all stations recorded sufficient occurrences of the different compound extremes to be included in the analysis.

For the assessment of the RCMs, models were compared to a gridded dataset of daily precipitation (Jones et al. 2013), and minimum and maximum temperature (Tencer et al. 2011) based on observed data at meteorological stations and developed during the CLARIS LPB project. The common domain covered by these datasets is 20–40° S, 45–70° W (see Fig. 1) in the period 1961–2000. Both the station data and the gridded datasets are available online at <http://wp32.at.fcen.uba.ar/>.

## 2.2. RCM simulations

Daily data from 7 RCM simulations from different institutions participating in the CLARIS LPB project were used in this study to assess the skill of the models to simulate the behaviour of the temperature and precipitation compound extreme events (Table 1). The domain of the models covers all of South America, bounded by 60° S–15° N and 90–20° (see Fig. 1), and simulations span the period 1990–2008. However, the area and period of study are constrained by the area covered by the observed gridded datasets to southeastern South America and 1990–2000 (see previous section and Fig. 1). All models were forced at the lateral boundaries and initial conditions by the ERA-Interim reanalysis (Simmons et al. 2007, Dee et al. 2011) at a horizontal resolution of approximately 50 km. Each model uses a different grid type, so they were re-interpolated to a common grid coincident with the observational dataset used for the intercomparison, based on a regular grid with a resolution of 0.5°. A correction by elevation was also applied to the simulated temperature using a standard lapse rate of 6.5°C km<sup>-1</sup> to take into account the topographical dif-

ferences between each native RCM grid and the observational grid. For more information on the simulations, re-interpolation method and an evaluation of the model performance in simulating seasonal means, see Solman et al. (2013).

## 2.3. Individual and compound extreme event definition

Based on the daily time series, warm days (nights) were defined as those days when maximum (minimum) temperature exceeded the 90th percentile of the empirical distribution of all days over a 5 d running window centred on each calendar day (Zhang et al. 2011). Cold days (nights) correspond to those days when maximum (minimum) temperature is below the 10th percentile of the empirical distribution, based on the same window of time. The 4 different types of extreme temperature events are referred to hereafter as Tx90 (warm days), Tn90 (warm nights), Tx10 (cold days) and Tn10 (cold nights).

Similarly, heavy precipitation events (hereafter Pr75) were defined as those days when the total accumulated daily rainfall exceeded the 75th percentile of the empirical distribution of rainy days (Pr > 0.1 mm), based on a 29 d moving window centred on each calendar day. The length of this window was selected to be longer than that recommended for temperature by the World Meteorological Organization Commission for Climatology/Climate Variability and Predictability/Joint Technical Commission for Oceanography and Marine Meteorology Expert Team on Climate Change Detection and Indices (ETCCDI; Zhang et al. 2011) due to the higher variability of daily precipitation compared to daily temperature.

Table 1. Regional climate models used in this study. See Table 1 in Solman et al. (2013) for more information on the models

Model	Institution	Reference
RCA 3.5	Rosby Centre, Swedish Meteorological and Hydrological Institute, Sweden	Samuelsson et al. (2010, 2011)
REMO 2009	Max-Planck-Institute for Meteorology, Hamburg, Germany	Jacob et al. (2001, 2012)
PROMES 2.4	Grupo MOMAC, Area Física de la Tierra, Facultad Ciencias Medio Ambiente, Universidad Castilla-La Mancha, Spain	Sanchez et al. (2007), Domínguez et al. (2010)
RegCM3	GrEC-USP, Departamento de Ciências Atmosféricas, Universidade de Sao Paulo, Brazil	Pal et al. (2007), da Rocha et al. (2009)
MM5 V3.7	Centro de Investigaciones del Mar y la Atmósfera, Argentina	Grell et al. (1994), Solman & Pessacg (2012)
LMDZ 4	Institute Pierre-Simon Laplace, France	Li (1999), Hourdin et al. (2006)
ETA Climate change V1.0	Instituto Nacional de Pesquisas Espaciais, Brazil	Pesquero et al. (2010), Chou et al. (2012)

A compound extreme event is defined in this study as the combined occurrence of 1 of the 4 temperature extremes and a heavy precipitation event. The occurrence of Pr75 can happen on the same day, the day before or the day after a temperature event. For each of these 3 cases and each compound extreme event (Pr75 combined with each of the 4 extreme temperature events defined above), the joint distribution was analysed using a contingency table with values  $n_{pt}$ , where  $p$  and  $t$  represent extreme precipitation and temperature events, respectively, and are represented by the numbers 1 or 2, indicating occurrence or non-occurrence, respectively, and  $n$  is the absolute frequency of occurrence of the compound event observed during the period of study. An independent contingency table was computed for the warm (October to March) and the cold season (April to September). The probability of Pr75 conditioned to the occurrence of a temperature extreme event is therefore given by  $n_{11}/(n_{11} + n_{21})$ , where  $n_{11}$  computes the number of days in the period when both types of extreme occurred, and  $n_{11} + n_{21}$  is the total amount of temperature extremes.

In the absence of a statistical relationship between these extremes, the conditional probability of Pr75 given the occurrence of a temperature extreme is equal to the probability of occurrence of Pr75 itself, which can be computed as the probability of having a rainy day multiplied by the probability of rainfall exceeding the 75th percentile, i.e. 0.25. We can therefore express the observed conditional probability of each compound extreme event as a ratio over the expected probability in the absence of a relationship. Ratios between 0 and 1 will depict a negative relation between the extremes, and therefore lower probability of heavy precipitation given that temperatures are extreme. Ratios  $>1$  describe a positive relation between extreme temperature and precipitation events, with the probability of heavy precipitation being increased by the occurrence of a temperature extreme.

The statistical significance of the relationship between temperature and extreme events was analysed at the 5% level by applying a 1-tailed chi-squared test (Wilks 2011). See Tencer et al. (2014) for details on the application of this test.

#### 2.4. Synoptic classification

In order to analyse the daily atmospheric circulation associated with compound extreme events, daily circulation patterns characterised by Barrucand et al.

(2014) were considered. The patterns were determined based on daily fields of 500 hPa geopotential heights over the domain 15–60° S and 40–90° W from NCEP Reanalysis II (Kanamitsu et al. 2002) for the reference period 1979–2008. The seasonality was removed by subtracting the daily average field over the reference period from each daily field.

Daily geopotential height anomalies at 500 hPa were synthesized using the principal component analysis technique, retaining the first 5 principal components that account for 82.2% of the total variance. A cluster analysis on the sub-space defined by these retained principal components was conducted using the  $k$ -means classification algorithm. This classification resulted in 10 dominant circulation types (labeled as CT $i$ , with  $i = 1 \dots 10$ ), which span the range of synoptic conditions over southern South America (see Fig. 5).

The comparison with some of the compound extreme events found in the present work required the utilization of daily fields of 500 hPa geopotential height from outside the reference period 1979–2008 used by Barrucand et al. (2014). Fields from the NCEP Reanalysis I (Kalnay et al. 1996) were used for events prior to 1979. Each one of these daily fields was projected onto the circulation patterns determined in the reference period and was assigned to the CT that correlated best with this field.

### 3. OBSERVED JOINT DISTRIBUTION OF EXTREME EVENTS

The analysis of the joint distribution of the simultaneous occurrence of warm nights and heavy precipitation events during the warm season (October to March; Fig. 2) shows a positive relationship between these 2 types of extremes over the entire region of study, i.e. the probability of occurrence of Pr75 increases during the occurrence of Tn90. This relationship is significant at the 5% level in  $>80\%$  of the stations and up to 3 times higher than expected in the absence of a statistical relation between the extremes in the SE subregion. The frequency of occurrence of Pr75 is also higher than expected on the day after Tn90 (Fig. 2e) in most of the region, although the relationship is slightly weaker than for the simultaneous case. However, when lagged in the opposite direction (Fig. 2i), the relation between these 2 extreme events becomes negative in all subregions except in the SE and parts of southern Chile (SW), indicating an inhibition of heavy precipitation events preceding a warm night. This could be related to the

fact that higher temperatures near the surface favour an increase in the amount of water vapour contained in the atmosphere and the thermodynamic instability that leads to convective activity that characterises this season of the year over the region (Re & Barros 2009). It is interesting to highlight that the region has experienced positive trends in warm nights in recent decades (Rusticucci & Barrucand 2004) and in heavy rainfall events (Re & Barros 2009, Penalba & Robledo 2010). Previous studies suggested that these increases are physically linked (Re & Barros 2009), which is in agreement with the strength of the relationship shown in Fig. 2a,e.

Warm days show a similar pattern when combined with Pr75 (Fig. 2), although there is more regionalization in the behaviour of this compound extreme for the simultaneous occurrence and when Pr75 happens on the day after Tx90 (Fig. 2e). However, for the case of Pr75 occurring before Tx90 (Fig. 2j), the whole study region presents a significant negative relationship, with almost no observed probability of occurrence of this compound extreme event when averaged over the entire region.

Cold nights are associated with an inhibition of heavy precipitation during the warm season, with only some exceptions for Pr75 preceding Tn10 in the NW subregion (Fig. 2k). Cold nights in the region are mainly related to anticyclones that lead to subsidence and weak surface winds together with low humidity and a clear sky (Müller et al. 2003), except for the NW region where local processes associated with mountain climates might prevail. Cold days can be associated with the occurrence of Pr75 on the same day (Fig. 2d) or the day before (Fig. 2l), but rarely on the day after (Fig. 2h), probably due to the passage of cold fronts.

Overall, the SW is the subregion with the fewest compound extreme events during the warm season and therefore with a less significant relationship between heavy precipitation and extreme temperature events. Stations in northern Chile do not contribute to this analysis due to the minimal occurrence of compound extreme events.

During the cold season (April to September, Fig. 3), the sign of the relationship between the different temperature extremes and Pr75 is usually the same as for the warm season, although the number of stations where the relation is significant is lower. The positive relationship between Tn90 and Pr75 observed in the SE is stronger, with probabilities of occurrence of Pr75 of more than 4 times greater than expected in the absence of a statistical simultaneous relationship. During the cold season, incursions of

tropical air into mid-latitudes are frequent and occur on the eastern side of the Andes, increasing temperature and atmospheric moisture over the region. This situation, combined with cyclogenesis during the transition seasons and synoptic activity during winter, could lead to the occurrence of warm nights and heavy precipitation events, especially over the SE subregion.

Figs. 2 & 3 demonstrate that the behaviour of the compound extreme events in each subregion east of the Andes responds to different climatic regimes, with clear differences between east and west, and north and south (see, for example, Fig. 3g or i).

#### 4. ATMOSPHERIC CIRCULATION ASSOCIATED WITH COMPOUND EXTREME EVENTS

After describing the statistical behaviour of observed compound extreme events in the previous section, we aim to characterise the general atmospheric circulation associated with them. For this purpose, the day of occurrence of each compound extreme event was identified at each location. Table 2 shows the number of days when >30% of the stations were affected by 1 particular compound extreme in each subregion (for this analysis, stations to the west of the Andes were not considered). In agreement with the results shown in Figs. 2 & 3, Tn90+Pr75 sub-regional events occurred more frequently than other compound extreme events in the NW, NE and SE regions, followed by Tx90+Pr75 events. Tx10+Pr75 occurred more frequently in the SW region.

In order to analyse whether the probability of occurrence of a compound event increases given the occurrence of a specific CT, the conditional probability of occurrence of a given compound event for a specific CT and the climatological probability of its occurrence were compared (as in Bettolli et al. 2010). The comparison was evaluated using the Z-test for a difference between 2 proportions under the null hypothesis that there is no difference between proportion values (Devore & Berk 2012). The test was performed only in cases when the sample size was sufficiently large, thus the Z-statistic followed a Gaussian distribution. The rejection of the null hypothesis, with a confidence level of 99%, indicates that the probability of occurrence of a compound event is enhanced when a given CT occurs.

Fig. 4 shows the percentage of compound extreme events associated with each CT for each subregion. The circulation pattern associated with Tn90+Pr75 depends on the subregion considered. The prob-

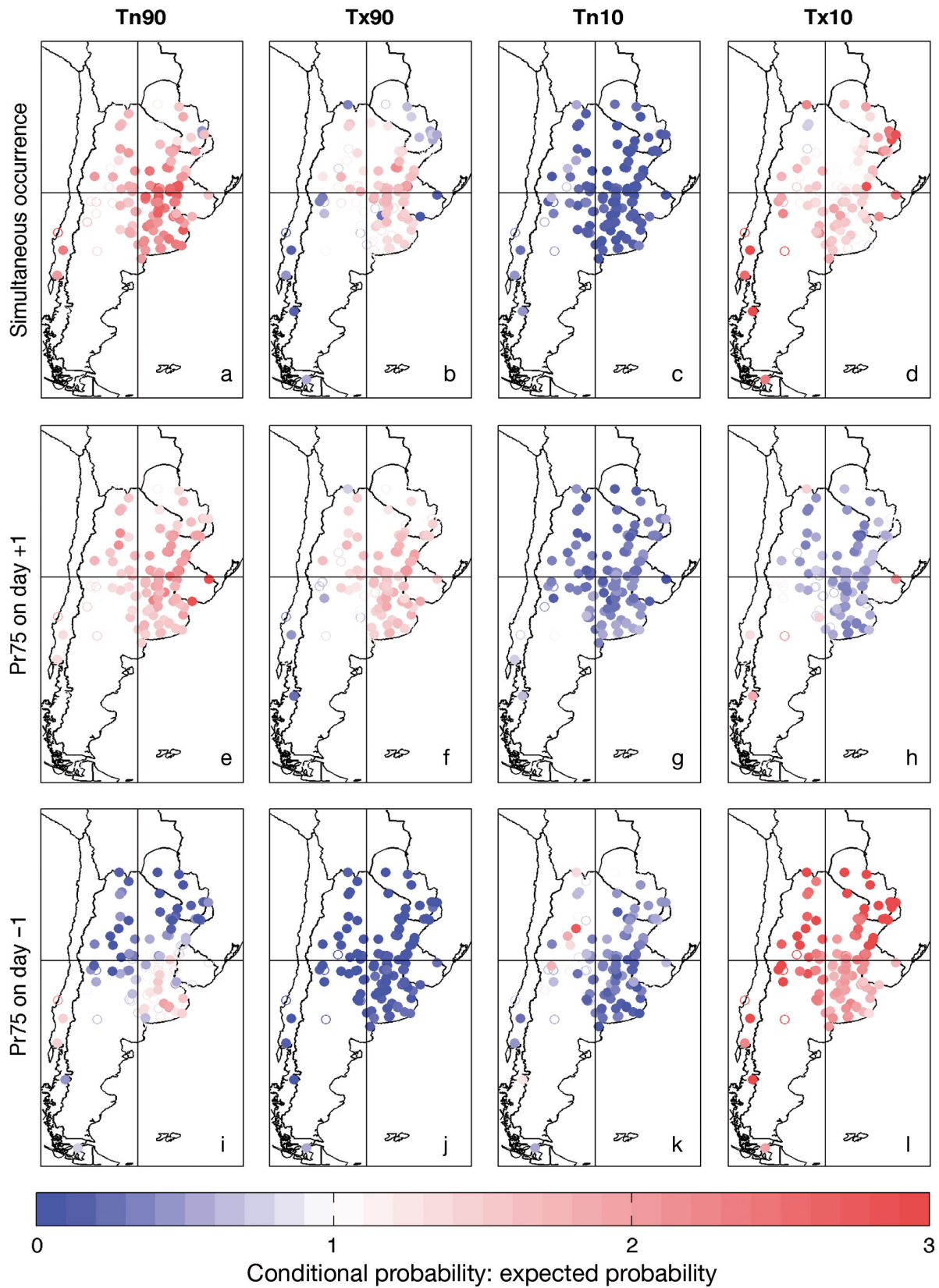


Fig 2. Heavy precipitation events occurring (a–d) simultaneously, (e–h) after or (i–l) before a temperature extreme event (Tn90, Tx90, Tn10, Tx10; see Table 2 for definitions) during the warm season (October to March) expressed as a ratio over the expected value (see Section 2.3 for details). Filled symbols depict a significant relationship at the 5% level

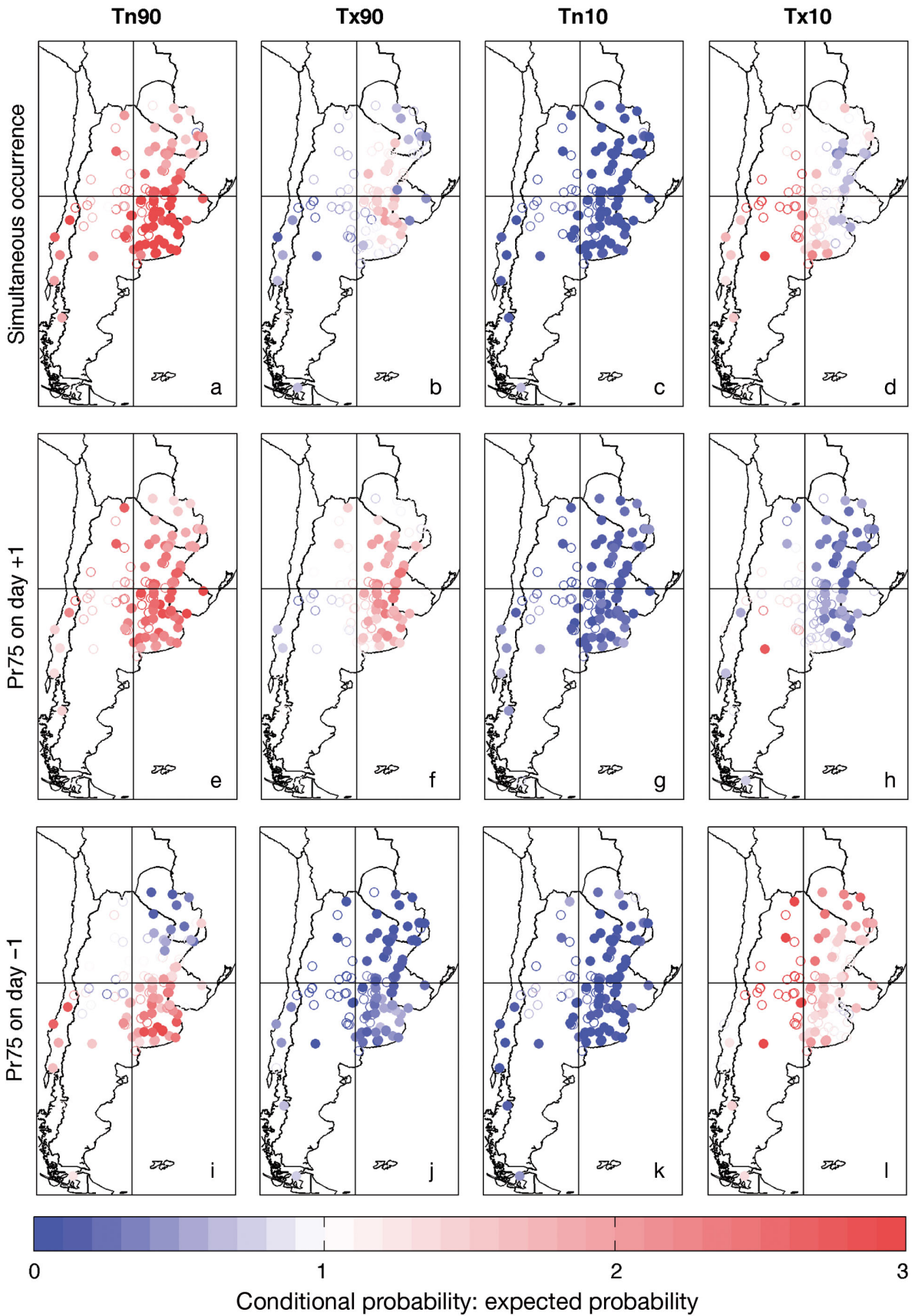


Fig. 3. Same as Fig. 2, but for the cold season (April to September)

ability of occurrence of this type of event is enhanced by the occurrence of CT8 over the NE, SE and SW subregions. This circulation pattern shows a short wavelength structure with a negative 500 hPa anomaly centred over the Pacific Ocean and a positive centre over the Atlantic Ocean at 40°S (Fig. 5). This structure is associated with a trough located in the subtropical sector of the Pacific Ocean with a surface cold front reaching low latitudes east of the Andes (not shown). The cold front is responsible for the warm and humid advection east of the front (NE and SE subregions) and for the forced rising motion that leads to heavy precipitation. These results are in agreement with Barrucand et al. (2014), who found that CT8 is inhibited during the opposite extreme events (cold and dry months). CT8 not only occurs simultaneously with Tn90+Pr75 but also the day before or the day after this compound event. When analysing surface circulation patterns, Penalba et al. (2013) found that heat waves in the region were dominated by the persistence of surface structures associated with CT8. The Tn90+Pr75 and Tx90+Pr75 events over the SE are also significantly favoured when CT1 dominates the circulation. This pattern shows a dipolar structure of geopotential height anomalies similar to CT8 but located farther south (with centres around 50–55°S), and consequently the associated disturbance favours warm and wet conditions mainly in the SE subregion.

The probability of occurrence of a Tn90+Pr75 event in the SE and SW subregions and Tx10+Pr75 in the SW are also significantly increased when CT5 dominates the circulation. This pattern is characterised by an anticyclonic centre located to the southeast of the continent which induces an anomalous easterly flow

Table 2. Absolute frequency of days when >30% of the stations in each subregion (east of the Andes) were affected by 1 particular compound extreme over the period 1961–2000. Tn90 (Tx90): minimum (maximum) temperature above the 90th percentile of the empirical distribution of all days over a 5 d running window centred on each calendar day; Tn10 (Tx10): minimum (maximum) temperature below the 10th percentile; Pr75: total accumulated daily rainfall above the 75th percentile of the empirical distribution of rainy days (Pr > 0.1 mm), based on a 29 d moving window centred on each calendar day

	Subregion			
	NW	NE	SW	SE
Tn90+Pr75	27	39	54	144
Tx90+Pr75	12	20	13	40
Tn10+Pr75	0	0	1	0
Tx10+Pr75	12	2	56	2

across the southern sector with enhanced moisture advection, needed for intense precipitation. High (low) minimum (maximum) temperatures are favoured by cloudiness that induces low radiative loss (gain) during the night (day).

CT10 significantly favours Tn90+Pr75 events over the SE and SW subregions. The configuration of this pattern has a centre of positive geopotential anomalies with a NW–SE axis extended from the Pacific Ocean to the Atlantic Ocean. This structure is associated with an upper level ridge and a perturbation positioned in Patagonia followed by a surface anticyclone centred southeast of Buenos Aires province

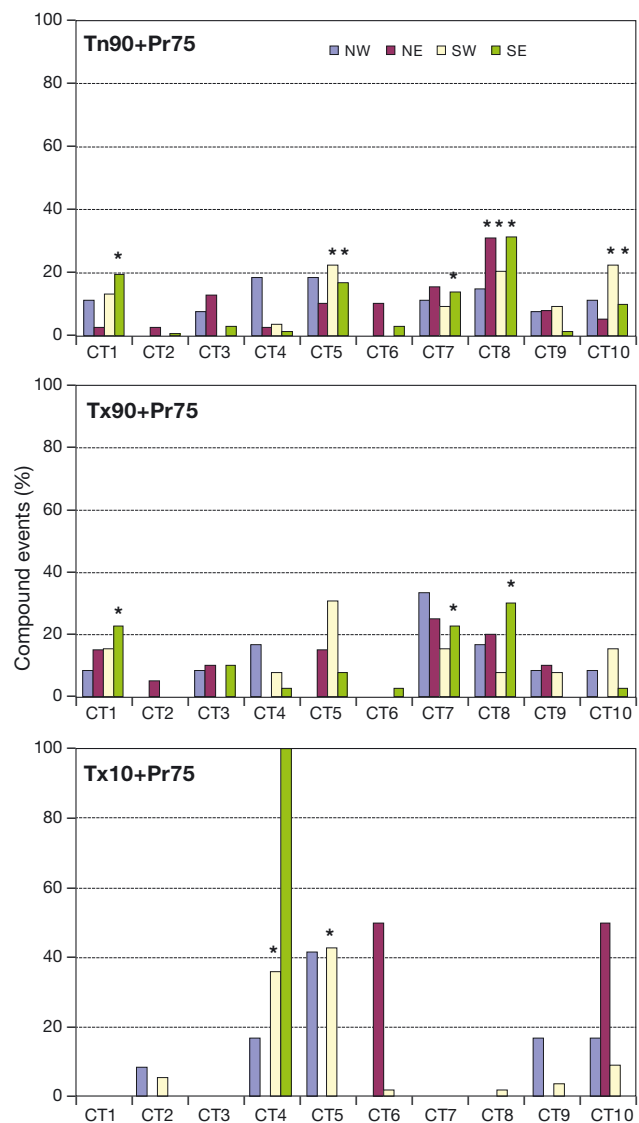


Fig. 4. Percentage of compound extreme events (see Table 2 for definitions) associated with each circulation type (CT; see Fig. 5) for each subregion (NE, NW, SE, SW; east of the Andes). \*Significant associations at the 1% confidence level

enhancing moisture, temperature and instability in the southern subregions (Fig. 5).

Tx90+Pr75 compound events exhibit fewer regionalized events than Tn90+Pr75. However, the analysis of the circulation associated with these events shows a predominant occurrence of the CT7 and CT8 patterns, being significant for the SE subregion. CT7 is characterised by a structure with a centre of negative anomalies positioned toward the extreme southwest tip of the continent extended over the Pacific Ocean and a centre of positive anomalies over the Atlantic Ocean, which extends towards the centre of the continent inducing anomalous flow from the northwest sector (Fig. 5). This pattern is associated with an intensification of the semi-permanent South Atlantic high, responsible for the high temperatures, and a frontal disturbance over the Patagonia region.

Cold and heavy precipitation days (Tx10+Pr75) show a smaller number of cases, except for the SW subregion (56 events, see Table 2). These compound events in the SW subregion are significantly associated with CT4 and CT5. CT4 is characterised by a high pressure system to the south of the continent, enhancing an anomalous flow from the east-southeast to the south of Argentina and a corresponding moisture advection at low levels. Low temperatures during the day could be related to cloudiness. CT4 and CT5 seem to show a sequence of the disturbance in its movement to the east (Fig. 5). For Tn10+Pr75, only 1 case was recorded in the 1961–2000 period (Table 2) in the SW region and was associated with CT10.

Heavy precipitation events and Tn90 or Tx10 show no association with some specific patterns, such as CT2. This result is consistent with the results found by Barrucand et al. (2014), who showed that CT2 is associated mainly with cold and dry months in central and northeastern Argentina.

It is interesting to highlight that 8 of the 14 significant associations (asterisks in Fig. 4) are found in the SE subregion. This could be due to the fact that in southern South America, incursions of both polar and tropical air masses are favoured along the eastern side of the Andes. This mountain range canalizes the flow, enhancing the meridional transport of air mass properties, mainly in the NE and SE. North of 40° S, cooling is the consequence of northward intrusions of cold fronts, and therefore warming in this region predominates when the frontal zone remains at higher latitudes (Barros et al. 2002). Moreover, advection of moisture could also be related to the easterly flow component from the Atlantic Ocean. On the other hand, situations that trigger precipitation processes

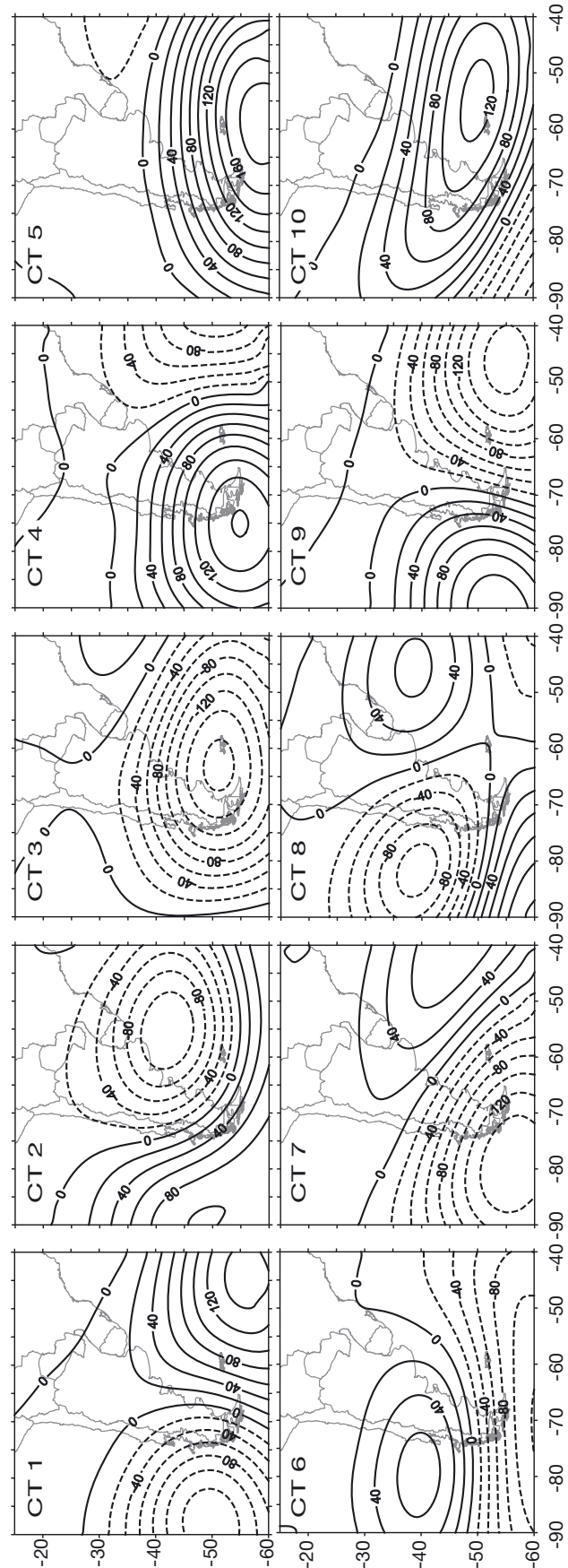


Fig. 5. Circulation types (CT): 500 hPa geopotential height anomalies (m). Adapted from Barrucand et al. (2014)

such as cyclogenesis and synoptic activity prevail in the southern subregions throughout the year, and particularly during the cold season. Therefore, conditions of high temperature (Tx90 and Tn90) and atmospheric moisture, together with forced rising motion due to synoptic disturbances seem to combine in the SE subregion, generating a greater response from compound events to CTs.

Regional compound events often occur in more than one subregion simultaneously and also in more than one condition. For example, on 9 September 1982, >30% of the stations in the SE and SW were affected by Tn90+Pr75 and Tx90+Pr75. On 7 September 1982, the circulation was dominated by a CT6 structure characterised by a disturbance entering from the Pacific Ocean and favouring a north component flow that initiates the advection of temperature and humidity over the region (see Fig. S1 in the Supplement, available at [www.int-res.com/articles/suppl/c068p183\\_supp.pdf](http://www.int-res.com/articles/suppl/c068p183_supp.pdf)). On 8 September 1982, a CT8 structure dominated the circulation, with the cold front positioned over the continent and the temperature and humidity anomalies increased over the SE and SW subregions. Some isolated compound events were registered on this day. On 9 September 1982, the CT8 structure persisted and enhanced the temperature and humidity anomalies east of the cold front that gave rise to simultaneous compound events over the region.

## 5. SIMULATED EXTREME EVENTS

### 5.1. Individual extremes

Before evaluating the models' skill to represent the distribution of compound extreme events, an assessment of their performance in simulating individual extremes is necessary. This analysis was made over the overlapping domain and period of the observed data and the model simulations, i.e. 1990–2000.

From the exploration of individual model performance, the spatial and temporal distributions of temperature extremes are well represented by the models (not shown). All models are able to simulate the highest values in the northern part of the domain and lower values at higher elevations along the Andes. Minimum temperature is generally better simulated, with spatial correlations between each model and the observations >0.9 and centred root mean square errors <1°C as shown in the Taylor diagrams (Taylor 2001) in Fig. 6. Overall, models tend to overestimate the spatial variability of Tn10 and Tn90 during the

warm season, and underestimate it in the cold season, as can be seen by the values of the normalized standard deviation in Fig. 6. In general, models overestimate Tn10 and Tn90 in most of the domain, except over the mountains to the west and on the northeast where some underestimation is observed. Mean differences between the multi-model ensemble and the observations over the entire domain are <2°C, with Tn90 showing slightly higher differences than Tn10, especially during the warm season (see Fig. S2 in the Supplement). These biases are higher than those found by Solman et al. (2013) for mean temperature over La Plata Basin during the austral winter using the same multi-model ensemble, although they used different observed datasets. They also reported a systematic underestimation of mean temperature throughout the year over the Andes, which is also seen in both extremes of minimum temperature. It is important to note here that observed gridded datasets may perform less accurately over regions of complex topography, such as the Andes (Tencer et al. 2011), and therefore some caveats should be considered when drawing conclusions regarding the skill of the models in these areas (Urrutia & Vuille 2009, Rauscher et al. 2010). During the warm season, biases tend to be slightly larger (around 3°C) over the whole domain.

Maximum temperature shows a greater spread among the models (Fig. 6) and lower spatial correlations (minimum correlation is 0.74). As for Tn, all models tend to overestimate the spatial variability within the domain. Centred root mean square errors are higher for Tx than for Tn, although still <1°C in most of the cases. A comparison between the multi-model ensemble and the observations during the warm season shows greater differences for warm than for cold extremes of Tx, with overestimation of the percentiles in the central part of the domain (up to 4°C for Tx90 and 2°C for Tx10, Figs. S3 & S5 in the Supplement) and underestimation in the west and northeast. During the cold season, the greater spread among the models leads to small differences between the ensemble and the observations (smaller than 2°C in most parts of the domain).

These biases indicate an improvement of the simulation of extreme temperature events in the region. Carril et al. (2012) reported warm biases of up to 8°C (6°C) for Tx90 (Tn10) when using previous versions of 4 of the 7 models used in this study (i.e. LMDZ, PROMES, RCA3 and REMO). However, the spatial pattern of the biases remains the same, with warm biases over La Plata Basin and cold biases over the mountainous regions to the west.

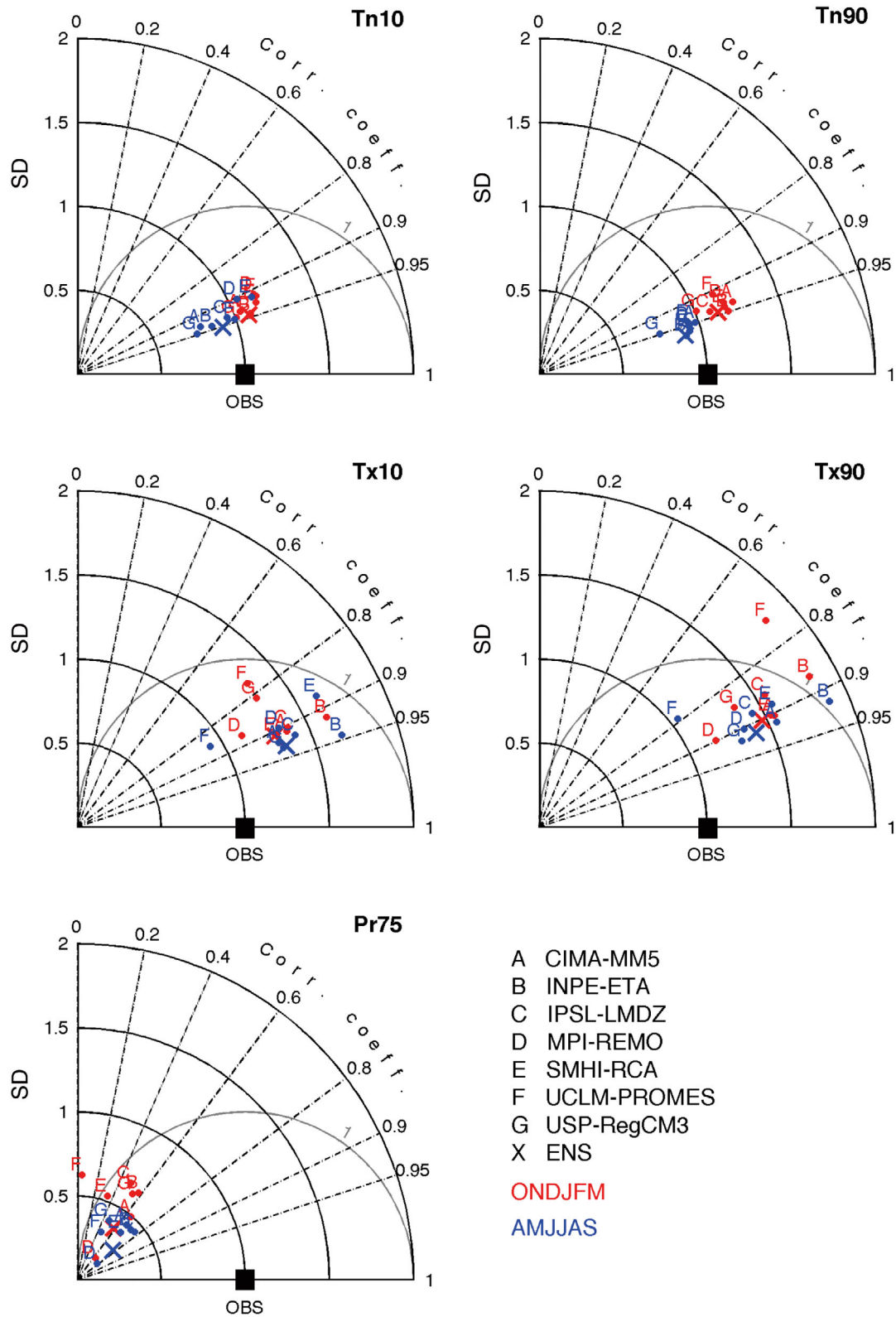


Fig. 6. Taylor diagrams for each individual extreme event analysed in this study for warm (red) and cold (blue) seasons (see Table 2 for definitions). Each point represents a model, and X is the ensemble of all models. Reference climatology (observations, OBS) is taken from Tencer et al. (2011) and Jones et al. (2013), described in Section 2.1. Standard deviation and centred root mean square errors are normalized by the observed standard deviation

All models underestimate Pr75, by >10 mm in some cases (Fig. S6), except in the northwest, where some overestimation is seen during the warm season. Even though models tend to underestimate Pr75 values, the spatial distribution of these events is well simulated. However, the correlation between observed and simulated Pr75 fields is <0.8 and spatial variability is underestimated in both seasons and by all models (Fig. 6). Mean differences between the model ensemble and the observations are around 6 mm over the entire domain (Fig. S6). In particular, the ensemble is able to localize the maximum intensity of Pr75 in April to September in southern Brazil and close to the coast, albeit with a large negative bias. This bias in the simulation of intense precipitation is in agreement with the negative biases found for mean precipitation during JJA over La Plata Basin by Solman et al. (2013), who reported differences >40% in the amount of monthly rainfall. During the warm season, they showed an underestimation of mean precipitation of around 15% and an overestimation over the upstream slopes of the Andes, which has also been reported before using other models (Rojas 2006, Urrutia & Vuille 2009). Both characteristics are present in the extreme values as well.

Overall, models tend to show warm and dry or cold and wet biases during the warm season, probably due to the strong dependence of these variables on model physics (Solman et al. 2013). This negative correlation between the 2 variables might have an impact on the occurrence of compound extreme events that has to be carefully considered in the analysis presented in the next section.

## 5.2. Compound extremes

In order to assess the skill of the RCMs to simulate the probability distribution of compound extreme events, we applied the same methodology described in Section 2.3 to each individual model and to a gridded observed dataset of daily temperature and precipitation (Tencer et al. 2011, Jones et al. 2013) over the common period 1990–2000. Even though individual extremes are not always perfectly simulated, especially for precipitation, the occurrence of compound extremes is defined relative to each model's representation of the individual extremes. Therefore, we can expect that the models are still able to capture the occurrence of the compound extremes. However, special care has to be taken into account due to the correlation between the

biases in temperature and precipitation, as mentioned in the previous section.

Fig. 7 shows the joint distribution of heavy precipitation and extreme temperature events for the warm season, as depicted by the observed dataset (upper panels) and the multi-model ensemble of 7 RCMs (lower panels) in southeastern South America. The resemblance between the upper panels of Figs. 7 & 2 is expected, since the gridded dataset is based on data observed at a subsample of the stations included in the analysis of Section 3. However, the negative simultaneous relationship only suggested by station data during the warm season between Pr75 and Tn90 in the NE subregion (Fig. 2a) and Tx10 in the NW subregion (Fig. 2d) are more evident when the gridded data are used.

Overall, models are in agreement with observations in simulating a direct relationship between heavy precipitation events and Tn90 in the southeastern part of the domain, and between Pr75 and Tx10 in the east and south, during the warm season. However, they fail to locate the regions of indirect relationships between these extremes. The opposite is found for Tx90, where models capture the negative relationship in most of the domain, but miss the positive relationship in the centre of the domain that is seen in the observations. For Tn10, the indirect relationship with Pr75 is well established in the entire domain, although the intensity of the simulated relationship is weaker than the observed values.

During the cold season, model performance is similar to the warm season. However, the smaller number of events observed and simulated during this time of the year makes the analysis less robust (not shown).

Fig. 8 shows a summary of the performance of each individual model and the multi-model ensemble for both seasons in the form of Taylor diagrams (Taylor 2001) for each compound extreme event. The spread among the models to reproduce the behaviour of the observed compound extremes is large in most of the cases, with negative spatial correlations in several cases, especially during the warm season. Overall, the multi-model ensemble (indicated by a cross in each panel) outperforms each individual model, mostly due to a compensation of biases among models. From the Taylor diagrams, we can conclude that the cold season is usually better represented than the warm season. However, the lower amount of compound events during April to September leads to less robust results.

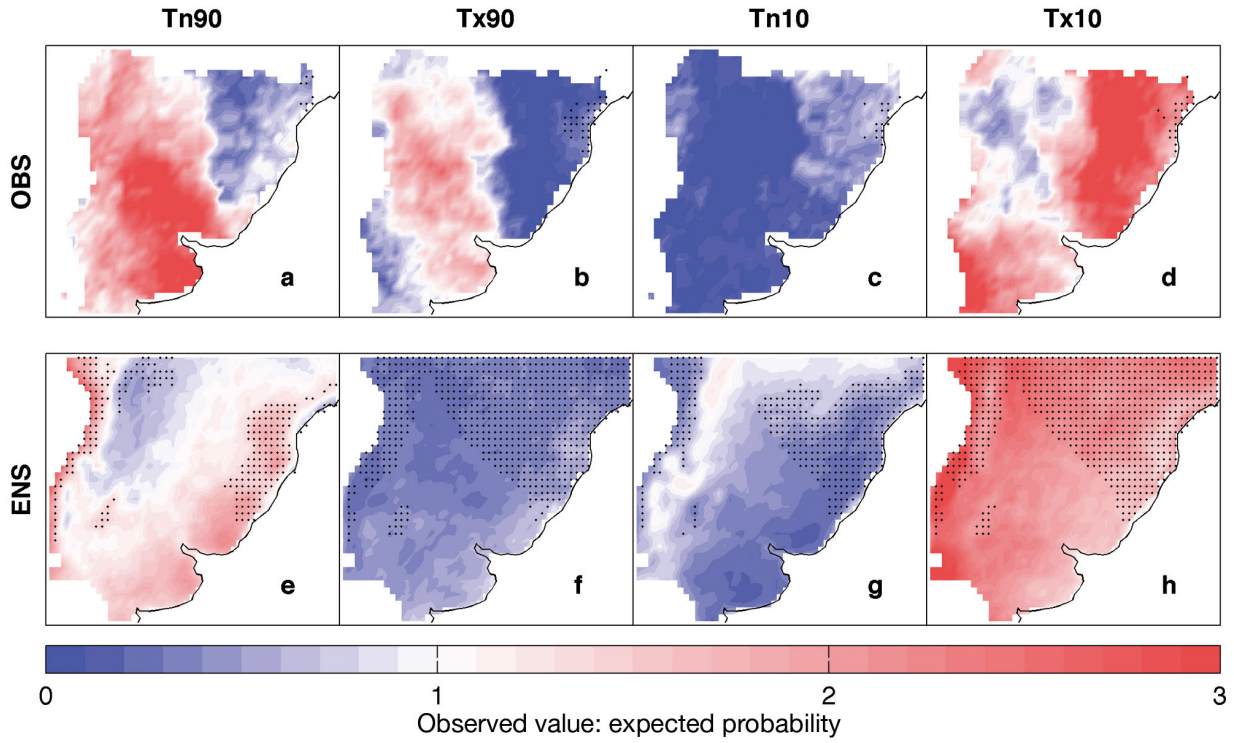


Fig. 7. Heavy precipitation events occurring together with a temperature extreme event (Tn90, Tx90, Tn10, Tx10; see Table 2 for definitions) during the warm season (October to March) expressed as a ratio over the expected value (see Section 2 for details) for (a–d) the observations and (e–h) the ensemble of all the models. Dots depict grid points with a significant relationship at the 5% level. The analysed domain corresponds to the red square in Fig. 1

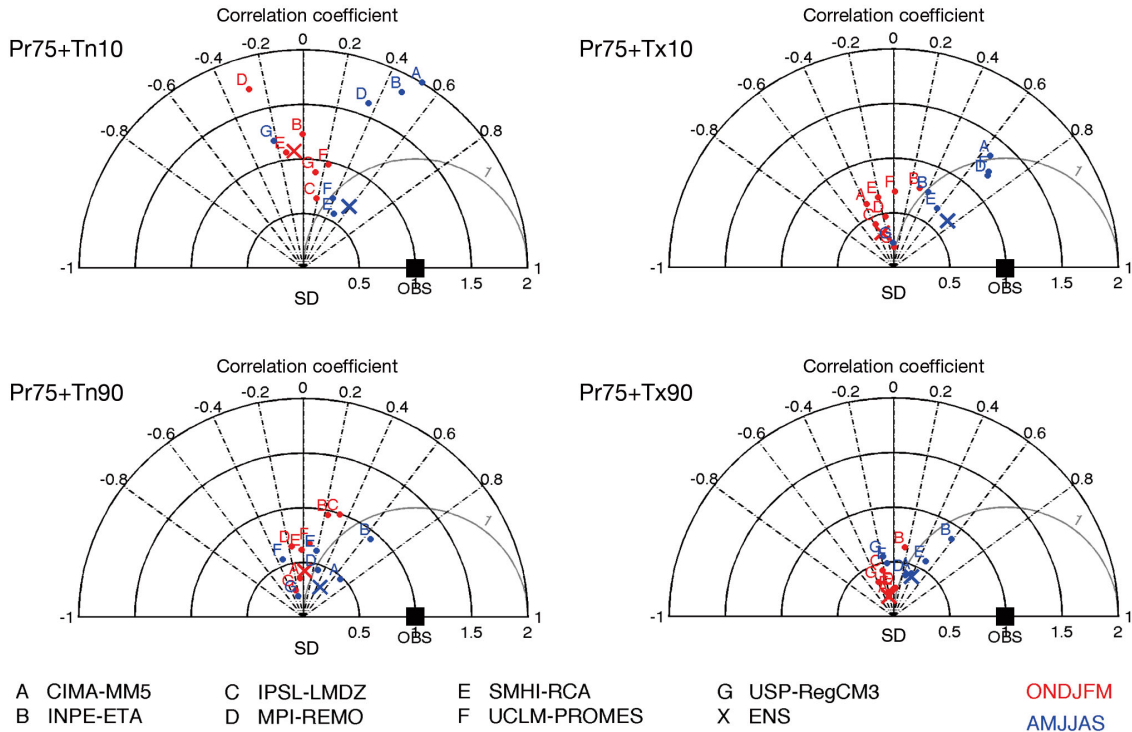


Fig. 8. Taylor diagrams for each compound extreme event for warm (red) and cold (blue) seasons (see Table 2 for definitions). Each point represents a model, and X is the ensemble of all models. Reference climatology (observations, OBS) is taken from Tencer et al. (2011) and Jones et al. (2013), described in Section 2.1. Standard deviation and centred root mean square errors are normalized by the observed standard deviation

## 6. CONCLUSIONS

In this paper, we have explored the statistical relationship between the occurrence of heavy precipitation events (defined as daily precipitation amounts exceeding the 75th percentile) and extreme temperatures (defined as daily minimum or maximum temperature above the 90th or below the 10th percentile) in southern South America during the period 1961–2000 and the atmospheric circulation associated with them.

We found that the occurrence of a warm night significantly increases the probability of occurrence of a heavy precipitation event on the same or the following day across the whole domain during the warm season, especially in the SE subregion. This type of compound event is more significantly associated with a circulation pattern characterised by a short wavelength structure at 500 hPa, with a negative anomaly over the Pacific Ocean and positive centre over the Atlantic near 40° S. At lower levels, a trough located in the subtropical Pacific Ocean and a cold front at lower latitudes east of the Andes advect warm and wet air to the eastern part of the domain.

The same pattern described above may also lead to the occurrence of extreme rainfall together with a warm day in the SE subregion. However, extreme rainfall amounts also occur more frequently than expected after a warm day, when a centre of negative anomalies is located in the southwestern tip of the continent and a positive anomaly lies over the Atlantic inducing anomalous northwest flow over the subregion.

The frequency of heavy precipitation events decreases with the occurrence of cold nights during the warm season in most of the region of study and after a cold day, but increases on the same day or the day before a cold day. More than two-thirds of heavy precipitation and cold days happen when a high pressure system is located at the south of the continent, enhancing the anomalous east-southeast flow responsible for the advection of moisture at low levels.

Even though it was not always possible to find one type of circulation pattern associated with each compound event, some of the patterns typically associated with drought conditions in the domain of study by Barrucand et al. (2014) were not associated with any of the compound extreme events analysed in this study, which correspond to intense precipitation.

A new generation of RCMs for the region was also evaluated in this paper with regards to their skills in simulating temperature and extreme precipitation events. The magnitude of biases in the simulation of

individual extremes has decreased compared to a previous version of 4 of the 7 models used in this study (compare results in Section 4.1 with Carril et al. 2012). However, biases of up to 2°C and underestimation of precipitation by >10 mm are still found between the ensemble of the models and the observed data. These biases are in agreement with results for mean values found by Solman et al. (2013), who reported a general negative correlation between mean temperature and precipitation biases during summer.

However, since compound extremes are defined relatively to each model's representation of individual extremes, these biases do not necessarily affect the skill of the models to simulate the joint distribution of heavy precipitation and temperature extreme events. In fact, we found an overall agreement between the simulations and the observed sign of the statistical relationship between these extremes in the region. Models were able to simulate an increase in the probability of occurrence of heavy rainfall during warm nights or cold days, and an inhibition of precipitation during cold nights. However, they tended to fail to capture the spatial pattern of the joint distribution of extreme temperature and precipitation events.

It is worth mentioning that the short period of time over which models and observations were compared (11 yr) could have influenced our assessment of the models. Results of this study should be extended over the whole period covered by the RCM simulations, for which an updated observed gridded dataset for the region is needed. It would also be useful to examine the circulation patterns during the occurrence of simulated compound extremes and their changes in future climate projections. We also aim to use the statistical relationship found between temperature and precipitation to evaluate changes in the occurrence of heavy precipitation events based on future projections of temperature extremes.

*Acknowledgements.* The research leading to these results received funding from the European Community's Seventh Framework Programme (FP7/2007-2013) under Grant Agreement No. 212492 (CLARIS LPB – A Europe-South America Network for Climate Change Assessment and Impact Studies in La Plata Basin). This work was also supported by CONICET Grant PIP0227 and UBA Grants 20020130100263BA and 20020130200142BA. Additional funding was provided by the Natural Sciences and Engineering Research Council of Canada (NSERC) CREATE Training Program in Interdisciplinary Climate Science. We thank the anonymous reviewers who helped improve the manuscript with their comments and suggestions.

## LITERATURE CITED

- Barros V, Grimm A, Doyle M (2002) Relationship between temperature and circulation in southeastern South America and its influence from El Niño and La Niña events. *J Meteorol Soc Jpn* 80:21–32
- Barrucand M, Vargas W, Bettolli ML (2014) Warm and cold dry months and associated circulation in the humid and semi-humid Argentina region. *Meteorol Atmos Phys* 123: 143–154
- Bettolli ML, Penalba OC (2014) Synoptic sea level pressure patterns—daily rainfall relationship over the Argentine Pampas in a multi-model simulation. *Meteorol Appl* 21: 376–383
- Bettolli ML, Penalba OC, Vargas W (2010) Synoptic weather types in the south of South America and their relationship to daily rainfall in the core production region of crops in Argentina. *Aust Meteorol Ocean J* 60:37–48
- Bradstock RA, Cohn JS, Gill AM, Bedward M, Lucas C (2009) Prediction and probability of large fires in the Sydney region of south-eastern Australia using fire weather. *Int J Wildland Fire* 18:932–943
- Carril A, Menéndez C, Remedio ARC, Robledo F and others (2012) Performance of a multi-RCM ensemble for South Eastern South America. *Clim Dyn* 39:2747–2768
- Chou SC, Marengo JA, Lyra A, Sueiro G and others (2012) Downscaling of South America present climate driven by 4-member HadCM3 runs. *Clim Dyn* 38:635–653
- da Rocha RP, Morales CA, Cuadra SV, Ambrizzi T (2009) Precipitation diurnal cycle and summer climatology assessment over South America: an evaluation of regional climate model version 3 simulations. *J Geophys Res* 114: D10108, doi:10.1029/2008JD010212
- Dee DP, Uppala SM, Simmons AJ, Berrisford P and others (2011) The ERA-interim reanalysis: configuration and performance of the data assimilation system. *Q J R Meteorol Soc* 137:553–597
- Devore JL, Berk KN (2012) *Modern mathematical statistics with applications*. Springer, New York, NY
- Domínguez M, Gaertner MA, de Rosnay P, Losada T (2010) A regional climate model simulation over West Africa: parameterization tests and analysis of land-surface fields. *Clim Dyn* 35:249–265
- Grell GA, Dudhia J, Stauffer DR (1994) A description of the fifth-generation Penn State/NCAR Mesoscale Model (MM5). NCAR Tech Note NCAR TN-398. National Center for Atmospheric Research, Boulder, CO
- Hourdin F, Musat I, Bony S, Braconnot P and others (2006) The LMDZ4 general circulation model: climate performance and sensitivity to parametrized physics with emphasis on tropical convection. *Clim Dyn* 27:787–813
- Jacob D, Van den Hurk BJJM, Andrae U, Elgered G and others (2001) A comprehensive model intercomparison study investigating the water budget during the BAL-TEX-PIDCAP period. *Meteorol Atmos Phys* 77:19–43
- Jacob D, Elizalde A, Haensler A, Hagemann S and others (2012) Assessing the transferability of the regional climate model REMO to different COordinated Regional Climate Downscaling EXperiment (CORDEX) regions. *Atmosphere* 3:181–199
- Jiang Y, Huang B (2000) Effects of drought or heat stress alone and in combination on Kentucky bluegrass. *Crop Sci* 40:1358–1362
- Jones PD, Lister DH, Harpham C, Rusticucci M, Penalba O (2013) Construction of a daily precipitation grid for southeastern South America for the period 1961–2000. *Int J Climatol* 33:2508–2519
- Kalnay E, Kanamitsu M, Kistler R, Collins W and others (1996) The NCEP/NCAR 40-Year Reanalysis Project. *Bull Am Meteorol Soc* 77:437–471
- Kanamitsu M, Ebisuzaki W, Woollen J, Yang SK, Hnilo JJ, Fiorino M, Potter GL (2002) NCEP-DOE AMIP-II Reanalysis (R-2). *Bull Am Meteorol Soc* 83:1631–1643
- Li L (1999) Ensemble atmospheric GCM simulation of climate interannual variability from 1979 to 1994. *J Clim* 12: 986–1001
- Madden RA, Williams J (1978) The correlation between temperature and precipitation in the United States and Europe. *Mon Weather Rev* 106:142–147
- Magrin GO, Marengo JA, Boulanger JP, Buckeridge MS and others (2014) Central and South America. In: Barros VR, Field CB, Dokken DJ, Mastrandrea MD and others (eds) *Climate change 2014: impacts, adaptation, and vulnerability. Part B. Regional aspects. Contribution of Working Group II to the Fifth Assessment Report of the Intergovernmental Panel on Climate Change*. Cambridge University Press, Cambridge, p 1499–1566
- Müller GV, Compagnucci R, Nuñez M, Salles A (2003) Surface circulation associated with frost in the wet Pampas. *Int J Climatol* 23:943–961
- Pal JS, Giorgi F, Bi X, Elquindi N and others (2007) The ITCP RegCM3 and RegCNET: regional climate modeling for the developing World. *Bull Am Meteorol Soc* 88: 1395–1409
- Penalba OC, Robledo FA (2010) Spatial and temporal variability of the frequency of extreme daily rainfall regime in the La Plata Basin during the 20th century. *Clim Change* 98:531–550
- Penalba OC, Bettolli ML, Krieger PA (2013) Surface circulation types and daily maximum and minimum temperatures in Southern La Plata Basin. *J Appl Meteorol Climatol* 52:2450–2459
- Penalba OC, Rivera JA, Pántano VC (2014) The CLARIS LPB database: constructing a long-term daily hydro-meteorological dataset for La Plata Basin, Southern South America. *Geosci Data J* 1:20–29
- Pesquero JF, Chou SC, Nobre CA, Marengo JA (2010) Climate downscaling over South America for 1961–1970 using the Eta model. *Theor Appl Climatol* 99:75–93
- Prohaska F (1976) The climate of Argentina, Paraguay and Uruguay. In: Schwerdtfeger W (ed) *Climates of Central and South America. World survey of climatology, Vol 12*. Elsevier Scientific Publishing Company, Amsterdam, p 13–72
- Rauscher S, Coppola R, Piani C, Giorgi F (2010) Resolution effects on regional climate model simulations of seasonal precipitation over Europe. *Clim Dyn* 35:685–711
- Re M, Barros VR (2009) Extreme rainfalls in SE South America. *Clim Change* 96:119–136
- Reisinger A, Kitching RL, Chiew F, Hughes L and others (2014) Australasia. In: Barros VR, Field CB, Dokken DJ, Mastrandrea MD and others (eds) *Climate change 2014: impacts, adaptation, and vulnerability. Part B. Regional aspects. Contribution of Working Group II to the Fifth Assessment Report of the Intergovernmental Panel on Climate Change*. Cambridge University Press, Cambridge, NY, p 1371–1438
- Rojas M (2006) Multiple nested regional climate simulations for southern South America: sensitivity to model resolution. *Mon Weather Rev* 134:2208–2223

- Rusticucci M, Barrucand M (2004) Observed trends and changes in temperature extremes over Argentina. *J Clim* 17:4099–4107
- Rusticucci M, Penalba OC (2000) Interdecadal changes in the precipitation seasonal cycle over Southern South America and their relationship with surface temperature. *Clim Res* 16:1–15
- Samuelsson P, Kourzeneva E, Mironov D (2010) The impact of lakes on the European climate as simulated by a regional climate model. *Boreal Environ Res* 15:113–129
- Samuelsson P, Jones C, Willén U, Ullerstig A and others (2011) The Rossby Centre regional climate model RCA3: model description and performance. *Tellus* 63:4–23
- Sanchez E, Gaertner MA, Gallardo C, Padorno E, Arribas A, de Castro M (2007) Impacts of a change in vegetation description on simulated European summer present-day and future climates. *Clim Dyn* 29:319–332
- Seneviratne SI, Nicholls N, Easterling D, Goodess CM and others (2012): Changes in climate extremes and their impacts on the natural physical environment. In: Field CB, Barros V, Stocker TF, Qin D and others (eds) *Managing the risks of extreme events and disasters to advance climate change adaptation. A special report of Working Groups I and II of the Intergovernmental Panel on Climate Change (IPCC)*. Cambridge University Press, Cambridge, p 109–230
- Simmons A, Uppala S, Dee D, Kobayashi S (2007) ERA-interim: new ECMWF reanalysis products from 1989 onwards. *ECMWF Newsl* 110:25–35
- Solman S, Pessacq N (2012) Regional climate simulations over South America: sensitivity to model physics and to the treatment of lateral boundary conditions using the MM5 model. *Clim Dyn* 38:281–300
- Solman S, Nuñez M, Cabré MF (2008) Regional climate change experiments over southern South America. I. Present climate. *Clim Dyn* 30:533–552
- Solman S, Sanchez E, Samuelsson P, da Rocha RP and others (2013) Evaluation of an ensemble of regional climate model simulations over South America driven by the ERA-Interim reanalysis: model performance and uncertainties. *Clim Dyn* 41:1139–1157
- Taylor KE (2001) Summarizing multiple aspects of model performance in a single diagram. *J Geophys Res* 106: 7183–7192
- Tencer B, Rusticucci M, Jones P, Lister D (2011) A southeastern South American daily gridded dataset of observed surface minimum and maximum temperature for 1961–2000. *Bull Am Meteorol Soc* 92:1339–1346
- Tencer B, Weaver A, Zwiers F (2014) Joint occurrence of daily temperature and precipitation extreme events over Canada. *J Appl Meteorol Climatol* 53:2148–2162
- Trenberth KE, Shea DJ (2005) Relationships between precipitation and surface temperature. *Geophys Res Lett* 32: L14703, doi:10.1029/2005GL022760
- Trenberth KE, Jones P, Ambenje P, Bojariu R and others (2007) Observations: surface and atmospheric climate change. In: Solomon S, Qin D, Manning M, Chen Z and others (eds) *Climate change 2007: the physical science basis. Contribution of Working Group I to the Fourth Assessment Report of the Intergovernmental Panel on Climate Change*. Cambridge University Press, Cambridge, p 235–336
- Urrutia R, Vuille M (2009) Climate change projections for the tropical Andes using a regional climate model: temperature and precipitation simulations for the end of the 21st century. *J Geophys Res* 114:D02108, doi:10.1029/2008JD011021
- Vera C, Silvestri G, Liebmann B, González P (2006) Climate change scenarios for seasonal precipitation in South America from IPCC-AR4 models. *Geophys Res Lett* 33: L13707, doi:10.1029/2006GL025759
- Wilks DS (2011) *Statistical methods in the atmospheric sciences*. Academic Press, San Diego, CA
- Zhang X, Alexander LV, Hegerl GC, Jones P and others (2011) Indices for monitoring changes in extremes based on daily temperature and precipitation data. *Wiley Interdiscip Rev Clim Chang* 2:851–870
- Zhao W, Khalil M (1993) The relationship between precipitation and temperature over the contiguous United States. *J Clim* 6:1232–1236

*Editorial responsibility: Filippo Giorgi, Trieste, Italy*

*Submitted: November 20, 2015; Accepted: April 8, 2016  
Proofs received from author(s): April 28, 2016*